DE LA RECHERCHE À L'INDUSTRIE

Werner Verdier[1] Alain Cartalade[1] Mathis Plapp[2]

[1]Université Paris-Saclay, CEA, Service de Thermo-hydraulique et de Mécanique des Fluides

[2]Laboratoire de Physique de la Matière Condensée, CNRS, École Polytechnique, Institut Polytechnique de Paris

April 5, 2023

Phase-field modelling and simulations of phase separation in the two-phase nuclear glass Na_2O–SiO_2–MoO_3

LBM Workshop, Institut Henri Poincaré

1 - Introduction

Context — nuclear glasses 1/2

Nuclear glasses

- Recyling of used nuclear fuel ⇒ nuclear waste.
- Containment of highly radioactive and long-lived nuclear waste with **nuclear glasses**.
- Best combinaison of thermal, chemical and radioactive isolation[9].
- Research on vitrification at CEA Marcoule and CEA project SIVIT.

Cold crucible at CEA Marcoule

[9] É. Vernaz and J. Bruezière. "History of Nuclear Waste Glass in France." In: *Procedia Materials Science* (2014)

Nucleation-growth phenomenology

- Processed to $\geq 1000°C \Rightarrow$ melting, crystallisation, **phase coexistence**
- Molybdenum-enriched waste incurs separation $\rightarrow$ model ternary glass $Na_2O-SiO_2-MoO_3$.

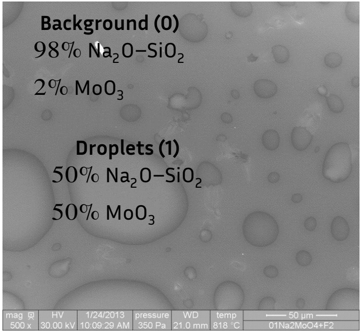

Ternary glass after liquid-liquid phase separation

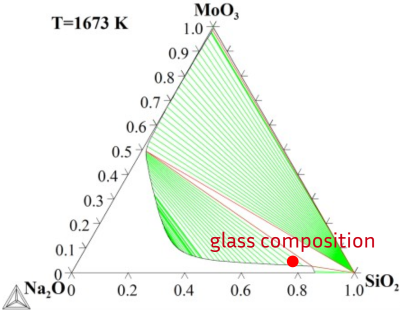

Phase diagram of the $Na_2O-SiO_2-MoO_3$

Scope and novelties

Scope

- Study kinematics of $Na_2O{-}SiO_2{-}MoO_3$ liquid-liquid interface in the growth regime (no spinodal decomposition)

Model requirements

- fully resolve the interface
- thermodynamic fidelity
- flow coupling
- high numerical efficiency

Novelties

- Simulations of binary growth usually done via Cahn-Hilliard formalism.
- We propose an alternate **phase-field (Allen-Cahn)** approach. Notably, consistent extension and thermodynamic data coupling in the ternary case.
- Includes hydrodynamics and all model eqs. are discretized using the **Lattice Boltzmann method**.
- High performance, portable simulation code **LBM_saclay**: simulations of many-droplets 3D growth.

2 - Model construction: ternary two-phase flow

Standard approach

Diffuse interface

- Usual formalism: Cahn-Hilliard equation
- Composition c used as order parameter
- Free energy functional $F[c]$ with intrinsic coupling of bulk and interface
- Under-determined in the ternary case!

Alternative: phase-field

- New order parameter φ to define the interface
- Therm. potential to define the bulk properties, interpolated in the interface using φ.
- Free energy functional $F[\varphi, c]$ with separate interface/bulk contributions.
- Consistent in the ternary case.

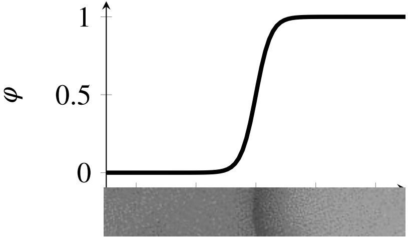

Diffuse interface between "phase 0" and "phase 1"

Phase-field basics 1/3

Free energy functional

$$F[\varphi, \mathbf{c}] = \int_V \mathrm{d}V \left(H f_{\mathrm{dw}}(\varphi) + \frac{\zeta}{2} |\nabla \varphi|^2 + f_{\mathrm{bulk}}(\varphi, \mathbf{c}) \right)$$

- $H f_{\mathrm{dw}}(\varphi) + \frac{\zeta}{2} |\nabla \varphi|^2$

Holds the diffuse interface's equilibrium profile and properties with double-well function

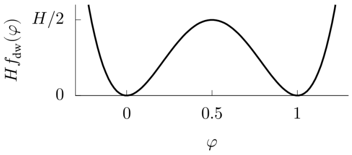

Double-well function $f_{\mathrm{dw}}(\varphi) = 8\varphi^2(1-\varphi)^2$

- $f_{\mathrm{bulk}}(\varphi, \mathbf{c})$

Thermodynamic energy contribution of the bulk phases w.r.t. thermodynamic field

$$\mathbf{c} = \begin{pmatrix} c^{SiO_2} & c^{Na_2O} \end{pmatrix}^T = \begin{pmatrix} c^A & c^B \end{pmatrix}^T$$

With $f_{\text{bulk}} = 0$,

- equilibrium profile, interface width and surface tension by minimization of $F[\varphi(x)]$

$$\varphi^{\text{eq}}(x) = \frac{1}{2}\left(1 + \tanh(2x/W)\right), \qquad W = \sqrt{\zeta/H}, \qquad \sigma^{\text{eq}} = \frac{2}{3}HW$$

- Time evolution PDE (Allen-Cahn equation)

$$\partial_t \varphi = -\frac{M_\varphi}{\zeta}\frac{\delta F[\varphi]}{\delta \varphi} \quad \Rightarrow \quad \partial_t \varphi = M_\varphi \nabla^2 \varphi - \frac{M_\varphi}{W^2} f'_{\text{dw}}(\varphi)$$

Only 2$^{\text{nd}}$ order space derivative (Cahn-Hilliard: 4$^{\text{th}}$).

Thermodynamic coupling via f_{bulk}

- Interpolate bulk phases's contribution

$$f_{\text{bulk}}(\varphi, \mathbf{c}) = p(\varphi) f_0(\mathbf{c}) + p(1-\varphi) f_1(\mathbf{c}) \qquad p(\varphi) = 3\varphi^2 - 2\varphi^3$$

$\Rightarrow$ tune $f_0(\mathbf{c})$,$f_1(\mathbf{c})$ (not f_{dw}!) to match real thermodynamic data (*eg*. Calphad)

- However, free energy not adequate for a chemical equilibrium.

Grand potential reformulation

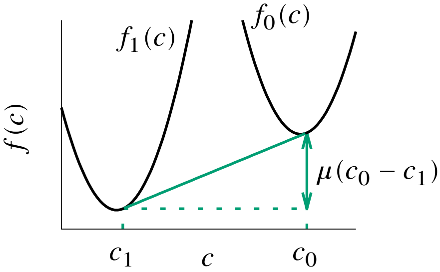

Binary common tangent construction

- Chemical eq. = common tangent plane construction.

$$\left.\frac{\partial f_0}{\partial \mathbf{c}}\right|_{\mathbf{c}_0} = \left.\frac{\partial f_1}{\partial \mathbf{c}}\right|_{\mathbf{c}_1} = \boldsymbol{\mu}$$

$$\underbrace{f_0(\mathbf{c}_0) - \boldsymbol{\mu}\cdot\mathbf{c}_0}_{\omega_0(\boldsymbol{\mu})} = \underbrace{f_1(\mathbf{c}_1) - \boldsymbol{\mu}\cdot\mathbf{c}_1}_{\omega_1(\boldsymbol{\mu})}$$

- Grand potential formalism[2]: use the Legendre transforms

$$\Omega[\varphi,\boldsymbol{\mu}] = \int \mathrm{d}V\,(\ldots + p(1-\varphi)\omega_0(\boldsymbol{\mu}) + p(\varphi)\omega_1(\boldsymbol{\mu}))$$

$$\omega_\pi(\boldsymbol{\mu}) = f_\pi(\mathbf{c}) - \boldsymbol{\mu}\cdot\mathbf{c} \qquad \mathbf{c} = -\frac{\delta\Omega}{\delta\boldsymbol{\mu}}$$

- The source term $p'(\varphi)(\omega_0(\boldsymbol{\mu}) - \omega_1(\boldsymbol{\mu}))$ is 0 at therm. eq.

[2] M. Plapp. “Unified derivation of phase-field models for alloy solidification from a grand-potential functional.” In: *Phys. Rev. E* (3 2011)

Two-phase ternary model

- Conservation of $\mathbf{c}$ by Onsager's variational principle

$$\partial_t c^\alpha = \nabla \cdot \mathbf{j}^\alpha, \qquad \mathbf{j}^\alpha = -M^\alpha(\varphi)\nabla\mu^\alpha$$

  mixed formulation[3] extended here to ternary[5]
- **Summary:** two-phase ternary model composed of
  1. φ interface tracking PDE,
  2. $\mathbf{c}$ diffusion PDE,
  3. closure relation $\mathbf{c} \leftrightarrow \boldsymbol{\mu}$ by Legendre transform.
- Missing ingredient: $f_\pi(\mathbf{c})$. How to define it?

[3] R. Bayle. "Simulation des mécanismes de changement de phase dans des mémoires PCM avec la méthode multi-champ de phase." 2020IPPAX035. PhD thesis. 2020

[5] W. Verdier. *Modèle à champ de phase pour verres ternaires diphasiques.* Note technique DES STMF/LMSF/NT/2021-67858 (CEA internal technical report). 2021

$Na_2O-SiO_2-MoO_3$ Calphad database

- Fit with Calphad data
- Numerical function $(T, c^{SiO_2}, c^{Na_2O}) \rightarrow \{f_\pi, \mu, c_\pi^{SiO_2,eq}, c_\pi^{Na_2O,eq}\}_{\pi=0,1}$

Calphad database

- $Na_2O-SiO_2-MoO_3$ ionic-liquid database[8]

$$\left(Mo^{4+},\ Na^{+}\right)_P$$

$$\left(MoO_4{}^{2-},\ O^{2-},\ SiO_4{}^{4-},\ MoO_3,\ O,\ SiO_2\right)_Q$$

Querying with OpenCalphad

- elements-to-oxides composition transform
- *Local equilibrium hypothesis* ⇒ turn off grid minimizer
- non-converging local equilibria are interpolated

[8] S. Bordier. "Modélisation thermodynamique des phases insolubles dans les verres nucléaires : application à la vitrification du molybdène et des produits de fission platinoïdes." 2015AIXM4339. PhD thesis. 2015

Choice of bulk free energies

- Simplest choice: convex elliptic wells

$$f_\pi(\mathbf{c}) = \frac{1}{2}\mathbf{K}_\pi : (\mathbf{c} - \mathbf{c}_\pi^{\mathrm{eq}})(\mathbf{c} - \mathbf{c}_\pi^{\mathrm{eq}})^T, \qquad \pi = 0, 1$$

  with symmetric positive definite matrices

$$\mathbf{K}_\pi = \begin{pmatrix} K_\pi^{\mathrm{SiO_2,SiO_2}} & K_\pi^{\mathrm{SiO_2,Na_2O}} \\ K_\pi^{\mathrm{Na_2O,SiO_2}} & K_\pi^{\mathrm{Na_2O,Na_2O}} \end{pmatrix} \qquad K_\pi^{\mathrm{SiO_2,Na_2O}} = K_\pi^{\mathrm{Na_2O,SiO_2}}$$

- Fit to thermodynamic data = setting the reference tie-line $(\mathbf{c}_0^{\mathrm{eq}}, \mathbf{c}_1^{\mathrm{eq}})$ and fitting the 2×3 matrix components.
- Extract characteristic energy scale k and define

$$\bar{\boldsymbol{\mu}} = \boldsymbol{\mu}/k \qquad \bar{\omega}_\pi = \omega_\pi/k \qquad \bar{\mathbf{K}}_\pi = \mathbf{K}_\pi/k \qquad \bar{M}^\alpha = kM^\alpha \qquad \lambda = H/k$$

Calphad fit example[7]

- 1. set global thermodynamic parameters

Temperature	1152 °C
SiO_2%	78.79%
Na_2O%	19.21%
MoO_3%	2%

- 2. free energy landscape via Calphad

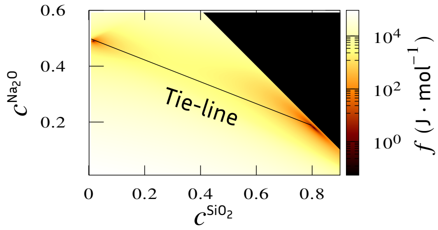

- 3. curve fit f_0, f_1 and obtain the $\mathbf{K}_\pi$ matrices.

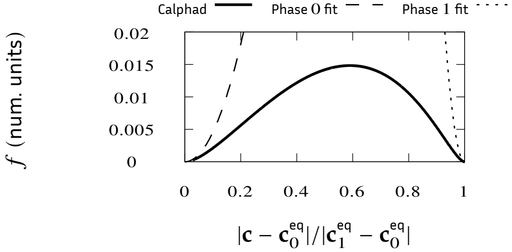

Fitted quadratics along tie-line

Concave part not fitted (grand potential) but not necessary (no spinodal decomposition)

[7] W. Verdier, R. Le Tellier, et al. "Coupling a grand potential ternary phase field model to the thermodynamic landscape of the Na2O-SiO2-MoO3 nuclear glass." In: *CALPHAD XLIX* (Skogshem & Wijk, Lidingö, May 22–27, 2022). 2022

- Convenient implicit representation of the interface, but implicit interface conditions!
- Asymptotic analysis w.r.t. "thinness" of W can reconstruct equivalent sharp-interface model

Gibbs-Thomson condition[6]

- local th. eq. perturbed by curvature κ and normal velocity V

$$\bar{\omega}_0 - \bar{\omega}_1 = -\delta\kappa - \beta V$$

with

$$\delta = \frac{2}{3}\frac{W}{\lambda} \qquad \beta = \frac{W}{M_\varphi}\left(\frac{2}{3}\frac{1}{\lambda} - \sum_\alpha \text{cte}\,\frac{M_\varphi}{M^\alpha}\left(\frac{\partial\omega_0}{\partial\mu^\alpha}\right)^2\right).$$

- Capillary length δ related to the surface tension,
- kinetic coefficient β typically made 0 by tuning λ.

[6] T. Boutin, W. Verdier, and A. Cartalade. "Grand-potential-based phase-field model of dissolution/precipitation: Lattice Boltzmann simulations of counter term effect on porous medium." In: *Computational Materials Science* (2022)

Coupling to hydrodynamics

Incompressible Boussinesq two-phase flow:

- advective terms $\mathbf{u} \cdot \nabla \varphi$ and $\mathbf{u} \cdot \nabla c^{\alpha}$, incompressible Navier-Stokes equations
- harmonic interpolation of phase viscosities, $\nu^{-1}(\varphi) = (1 - \varphi)\nu_0^{-1} + \varphi \nu_1^{-1}$
- buoyancy force under Boussinesq approximation and linear densities interpolation
- capillary force $\propto \sigma \kappa$ normal to the interface

Phase field model PDEs with flow

Legendre transforms

$$f_\pi(\mathbf{c}) \to \bar{\omega}_\pi(\bar{\boldsymbol{\mu}}) = -\frac{1}{2}\bar{\mathbf{K}}_\pi^{-1} : \bar{\boldsymbol{\mu}}\bar{\boldsymbol{\mu}}^T - \mathbf{c}_\pi^{\mathrm{eq}} \cdot \bar{\boldsymbol{\mu}}, \qquad \bar{\boldsymbol{\mu}} = \bar{\mathbf{K}}(\varphi)(\mathbf{c} - \mathbf{c}^{\mathrm{eq}}(\varphi))$$

PDE system (discretized by lattice Boltzmann method)

- Interface-tracking

$$\partial_t \varphi + \mathbf{u} \cdot \nabla \varphi = M_\varphi \nabla^2 \varphi - \frac{M_\varphi}{4W^2}\varphi(1-\varphi)(\frac{1}{2} - \varphi) - \frac{\lambda M_\varphi}{W^2} 6\varphi(1-\varphi)(\bar{\omega}_0(\bar{\boldsymbol{\mu}}) - \bar{\omega}_1(\bar{\boldsymbol{\mu}}))$$

- Component diffusion

$$\partial_t c^\alpha + \mathbf{u} \cdot \nabla c^\alpha = \nabla \cdot \bar{M}^\alpha \nabla \bar{\mu}^\alpha \qquad \text{for } \alpha = SiO_2, Na_2O$$

- Averaged two-phase flow

$$\nabla \cdot \mathbf{u} = 0 \qquad \rho \partial_t \mathbf{u} + \rho \nabla \cdot (\mathbf{u}\mathbf{u}^T) = \rho \nabla \cdot \left[\nu(\varphi)(\nabla \mathbf{u} + \nabla \mathbf{u}^T)\right] - \nabla p + \varphi \Delta \rho \mathbf{g} - \frac{\sigma}{W}\boldsymbol{\kappa}(\varphi)$$

3 - Numerical implementation

Lattice Boltzmann method

- Solves a Boltzmann equation in a discrete velocity space.
- Timestep algorithm: collision and transport of discrete distribution functions on a lattice.
- Reconstruct diffusion or hydrodynamics equations ⇒ all-LBM scheme for our model.
- GPU friendly: collision is memory-local, transport along regular memory stencil

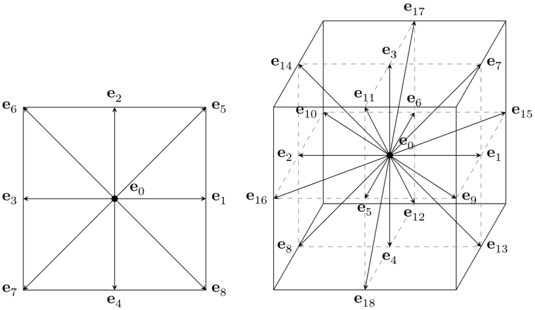

D2Q9 and D3Q19 discretization lattice.

Lattice Boltzmann equations of the model

- The continuum equations already handle all the complexities of the two-phase system (interface geometry, interface conditions, interpolations...)
- The discretisation is kept at its simplest: 4 separate LBM-BGK equations (flow, phase-field, A and B diffusion).

Lattice Boltzmann equations – hydrodynamics

$$v_k(t+\delta t, \mathbf{x}+\delta x \mathbf{e}_k) = \left(1 - \frac{1}{\bar{\tau}_v}\right) v_k(t,\mathbf{x}) - \frac{1}{\bar{\tau}_v} v_k^{\text{eq}}(t,\mathbf{x}) + \delta t S_{v,k}(t,\mathbf{x}),$$

with

$$\bar{\tau}_v(\varphi) = \frac{\nu(\varphi)}{\delta t c_s^2} + \frac{1}{2},$$

$$v_k^{\text{eq}} = w_k p + (\gamma_k - w_k)\rho c_s^2 - \frac{\delta t}{2} S_{v,k},$$

$$S_{v,k} = \gamma_k\,(\mathbf{c}_k - \mathbf{u}) \cdot \left(\varphi \Delta \rho \mathbf{g} - \frac{\sigma}{W}\boldsymbol{\kappa}(\varphi)\right).$$

Reconstructed moments:

$$p = \sum_k v_k,$$

$$\mathbf{u} = \frac{1}{\rho {c_s}^2}\left(\sum_k \mathbf{c}_k v_k + \frac{\delta t}{2} c_s^2 \left(\varphi \Delta \rho \mathbf{g} - \frac{\sigma}{W}\boldsymbol{\kappa}(\phi)\right)\right).$$

Lattice Boltzmann equations – phase field

$$h_k(t+\delta t, \mathbf{x}+\delta x \mathbf{e}_k) = \left(1-\frac{1}{\bar{\tau}_h}\right) h_k(t,\mathbf{x}) + \frac{1}{\bar{\tau}^h} h_k^{\text{eq}}(t,\mathbf{x}) + \delta t S_{h,k},$$

where

$$\bar{\tau}_h = \frac{M_\varphi}{\delta t c_s^2} + \frac{1}{2},$$

$$h_k^{\text{eq}} = w_k \varphi \left(1 + \frac{\mathbf{c}_k \cdot \mathbf{u}}{c_s^2}\right) - \frac{\delta t}{2} S_{h,k},$$

$$S_{h,k} = w_k \frac{M_\varphi}{W^2} \left(-f_{\text{dw}}(\varphi) + \lambda p'(\varphi) \Delta\bar{\omega}(\bar{\mu}^A, \bar{\mu}^B)\right).$$

Moment:

$$\varphi = \sum_k h_k + \frac{\delta t}{2} \frac{M_\varphi}{W^2} \left(-f_{\text{dw}}(\varphi) + \lambda p'(\varphi) \Delta\bar{\omega}(\bar{\mu}^A, \bar{\mu}^B)\right).$$

Lattice Boltzmann equations – chemical diffusion

$$a_k(t+\delta t, \mathbf{x}+\delta x \mathbf{e}_k) = \left(1 - \frac{1}{\bar{\tau}^a}\right) a_k(t,\mathbf{x}) + \frac{1}{\bar{\tau}^a} a_k^{\mathrm{eq}}(t,\mathbf{x}),$$

$$b_k(t+\delta t, \mathbf{x}+\delta x \mathbf{e}_k) = \left(1 - \frac{1}{\bar{\tau}^b}\right) b_k(t,\mathbf{x}) + \frac{1}{\bar{\tau}^b} b_k^{\mathrm{eq}}(t,\mathbf{x}),$$

with

$$\bar{\tau}^a = \frac{\bar{M}^{AA}(\varphi)}{\delta t c_s^2} + \frac{1}{2}, \qquad a_k^{\mathrm{eq}} = \begin{cases} w_k \left(3\Gamma \bar{\mu}^A + c^A \dfrac{\mathbf{c}_k \cdot \mathbf{u}}{c_s^2}\right), & k \neq 0, \\ c^A - 3\Gamma(1-w_0)\bar{\mu}^A, & k = 0, \end{cases}$$

$$\bar{\tau}^b = \frac{\bar{M}^{BB}(\varphi)}{\delta t c_s^2} + \frac{1}{2}, \qquad b_k^{\mathrm{eq}} = \begin{cases} w_k \left(3\Gamma \bar{\mu}^B + c^B \dfrac{\mathbf{c}_k \cdot \mathbf{u}}{c_s^2}\right), & k \neq 0, \\ c^B - 3\Gamma(1-w_0)\bar{\mu}^B, & k = 0, \end{cases}$$

Moments:

$$c^A = \sum_k a_k, \qquad c^B = \sum_k b_k.$$

- Development of a high-performance Lattice Boltzmann simulation code: LBM_saclay
- Portable on multi-CPU/GPU architectures of modern supercomputers
- Shared-memory parallelism with the Kokkos C++ library, distributed-memory with MPI.

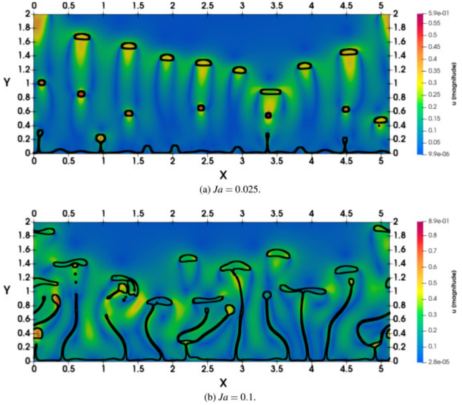

Phase-field film boiling simulations simulated with LBM_saclay[1]. 4096×3072, ~80 minutes with 8 K80 GPUs

[1] W. Verdier, P. Kestener, and A. Cartalade. "Performance portability of lattice Boltzmann methods for two-phase flows with phase change." In: *Computer Methods in Applied Mechanics and Engineering* (2020)

Performance portability

- LBM_saclay builds on desktop workstations, multi-CPU clusters or multi-GPUs supercomputers from the same unmodified source code.
- Enabled by the Kokkos[11] C++ library: shared-memory parellelism with pthreads/OpenMP/CUDA depending on build system switches.
- **Performance** portability: can still tweak finer details at compile-time for each arch.

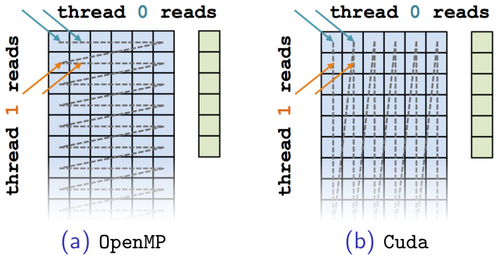

Different array CPU/GPU array memory layout for better memory coalescence taken from Kokkos tutorial slides

[11] H. C. Edwards, C. R. Trott, and D. Sunderland. "Kokkos: Enabling manycore performance portability through polymorphic memory access patterns." In: *Journal of Parallel and Distributed Computing* 12 (2014). Domain-Specific Languages and High-Level Frameworks for High-Performance Computing

LBM_saclay 3/3

Initial prototype

- advec.-diff. and simple two-phase flows,
- periodic and bounceback (Neumann) conditions,
- untested on large 3D simulations.

Developments during the thesis

- capillary force, boiling flow, **two-phase ternary flow for glasses** (with WIP Calphad coupling)
- fixes on the bounceback conditions (“half-way” bounceback), anti-bounceback (Dirichlet)
- reworked the MPI communications (communicate macro. var.)
- first version of HDF5 outputs
- stress tested on the **Jean-Zay GPU supercomputer**
- + high-performance post-processing...

4 - Simulations

Intermediate validations 1/3

- **Double Poiseuille test-case** — validation of the flow sub-model

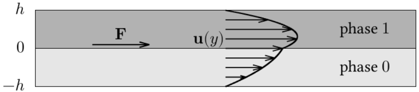

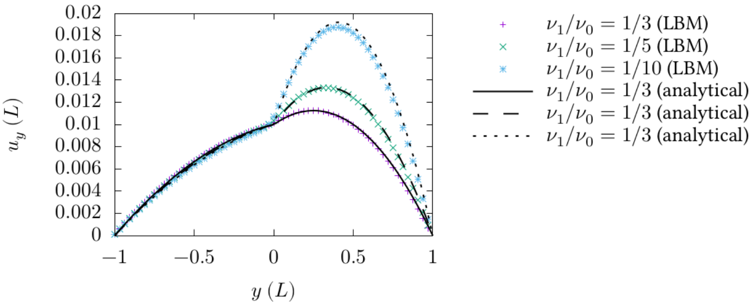

Intermediate validations 2/3

- **Ternary diffusion couple test-case** — validation of the two-phase three-component sub-model

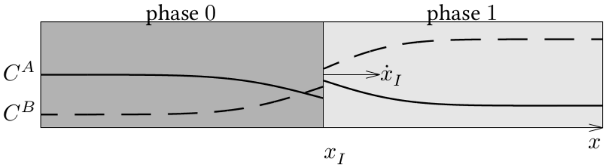

- Displacement of a plane interface by diffusion
- Test the diffuse–sharp interface aymptotic equivalence. Must reconstruct
  - discontinuous interface $\mathbf{c}$, continuous interface $\boldsymbol{\mu}$
  - displacement $x_I(t) \propto \sqrt{t}$.

Intermediate validations 3/3

- Comparison against analytical solutions
- Non-fitted $\mathbf{K}$ matrices (num. stability issues)

$x_I(t) \propto \sqrt{t}$

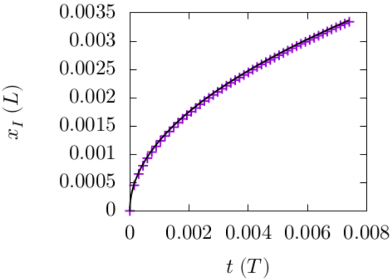

erfc composition profiles

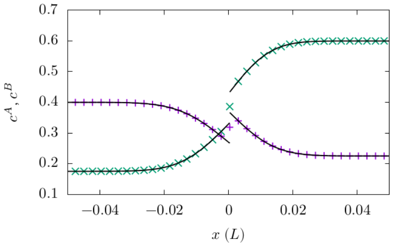

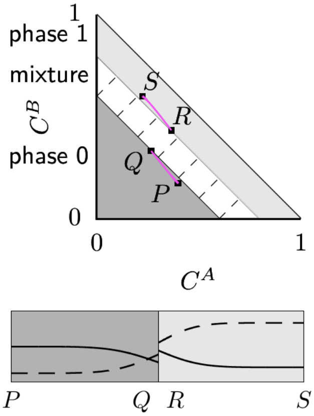

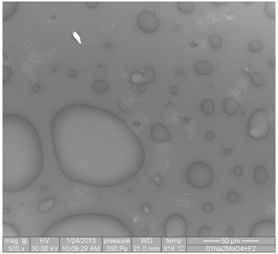

Modeling the growth kinetics

- Gibbs-Thomson condition: $|\boldsymbol{\mu} - \boldsymbol{\mu}^{\text{eq}}| \sim 2\delta/R$

  larger droplets have lower chemical potential
- Component diffusion flux: $\mathbf{j} \sim -\nabla\boldsymbol{\mu}$

  migration from smaller, vanishing droplets to larger, growing droplets
- Expected mean radius[4]: $\langle R\rangle(t) \propto t^p$

  with $p = 1/3$ without flow, $= 1$ with flow, > 1 with buoyancy.

Initial conditions

- No concave f: must start from pre-nucleated droplets

[4] E. D. Siggia. "Late stages of spinodal decomposition in binary mixtures." In: *Phys. Rev. A* (2 1979)

Simulations of droplet growth 2/4

- Purely diffusive, without flow.
- Start from a nucleated initial condition (~ 3000 droplets)
- After a transient regime we observe the power-law of $\langle R \rangle (t)$, homogeneization of μ.

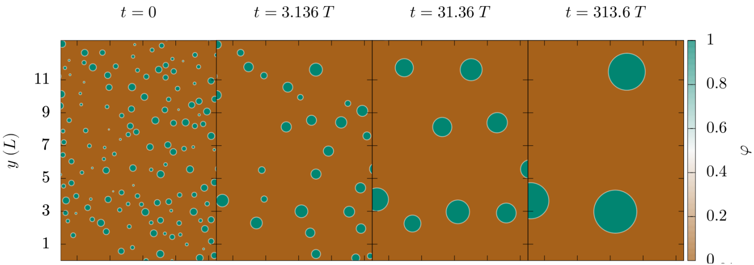

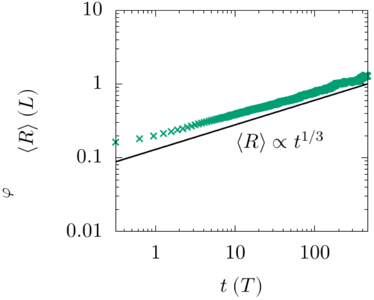

Simulations of droplet growth 3/4

- Large 3D simulation to stress test future exp. observations: 2048×512×512, ~20 hours with 16 V100 GPUs (Jean-Zay).
- Flow with sedimentation — might be relevant with high MoO_3 composition

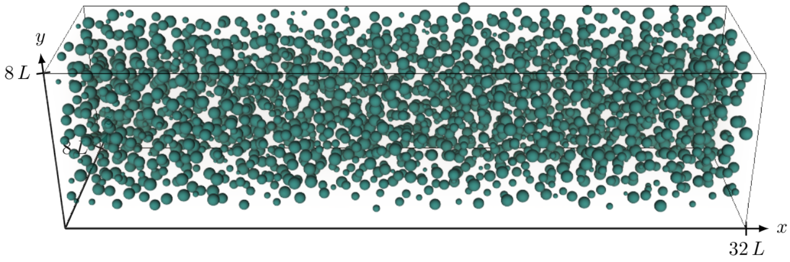

Initial condition (~2000 droplets)

Simulations of droplet growth 4/4

- With a 3D buoyancy-accelerated flow, we start seeing the > 1 cross-over.
- Buoyancy accelerates larger droplets $\Rightarrow$ accelerates coalescence

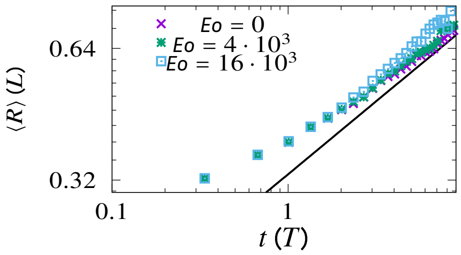

Evolution of the droplet mean radius

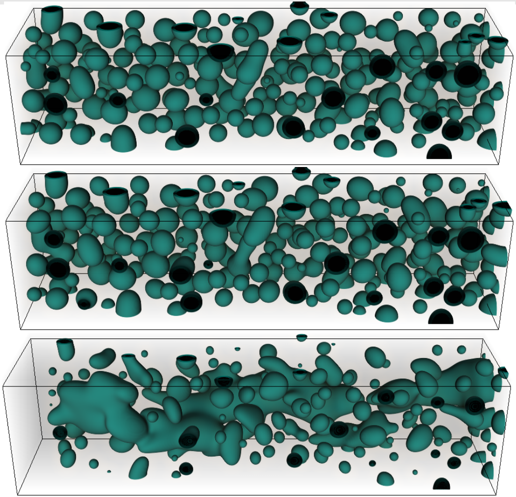

Final timestep with $Eo = 0$ (top), $Eo = 4 \cdot 10^3$ (middle), $Eo = 16 \cdot 10^3$ (bottom).

Simulations of droplet growth 4/4

- With a 3D buoyancy-accelerated flow, we start seeing the > 1 cross-over.
- Buoyancy accelerates larger droplets $\Rightarrow$ accelerates coalescence

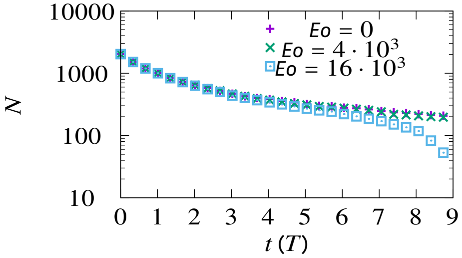

Evolution of the droplet crount

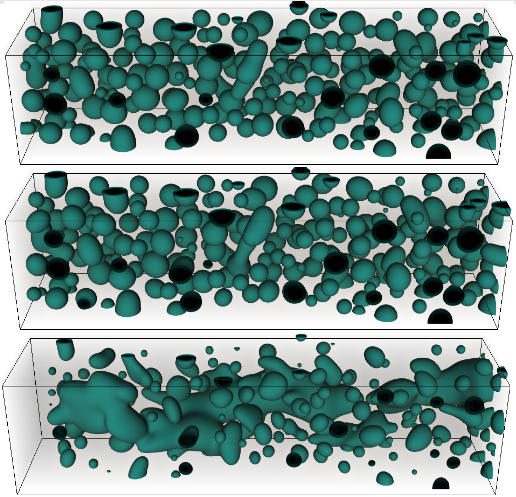

Final timestep with *Eo* $= 0$ (top), *Eo* $= 4 \cdot 10^3$ (middle), *Eo* $= 16 \cdot 10^3$ (bottom).

5 - Conclusion

Conclusion

Summary & results

- Established a model for the kinetics of a liquid-liquid interface in a nuclear glass
- Developed a high performance numerical simulation code (LBM_saclay) and carried out intermediate validations of the model
- Showed it reproduce the power-law growth regime with flow and sedimentation effects
- Coupling to Calphad data established and implemented

Perspectives

- model: “cleaner” hydrodynamic coupling $\Omega[\varphi, \boldsymbol{\mu}, p, \mathbf{u}]$
- numerical: better LBM collision term to improve stability
- but more immediately...

Conclusion

- ... comparison to experimental observations carried out at CEA Marcoule.

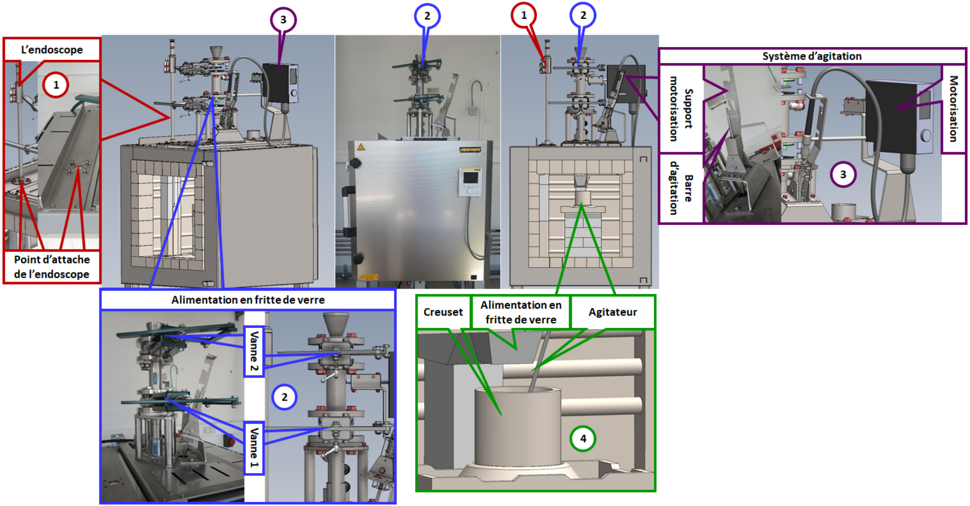

Acknowledgements

- Pierre Kestener (CEA Saclay), first prototype of LBM_saclay
- Romain Le Tellier (CEA Cadarache, SIVIT), experience on phase-field-Calphad coupling
- Stéphane Gossé and Paul Fossati (CEA Saclay, SIVIT), Calphad $Na_2O-SiO_2-MoO_3$ database
- Experimentalists at LDPV and LM2T (CEA Marcoule, SIVIT), future experimental application
- Sophie Schuller (CEA Marcoule), head of project SIVIT
- Industrial partners of SIVIT: Orano, EDF.

Thank you for your attention.

Simulation of droplet ripening (Calphad coupling)

Work in progress

- Simulations with fitted $\mathbf{K}_i$ diverge at long times
- Orders of magnitudes between $\mathbf{K}_i$ values ⇒ different num. stability ranges
- Additional conditions on $\mathbf{D}$ (symmetrical, interpolation between phases)

⇒ a few adjustments on the LBM discretization and/or phase field interpolations (or find an easier equilibrium)

$$M^\alpha \nabla \mu^\alpha \cong \underbrace{M^\alpha \sum_{\beta=\mathrm{Na_2O,SiO_2}} K(\varphi)^{\alpha\beta}}_{\mathbf{D}(\varphi)} \nabla c^\beta$$

phase	$\mathbf{K}_i$ matrix	eigenvalues
background (0)	$\begin{pmatrix} 4.38 & 4.79 \\ 4.79 & 5.49 \end{pmatrix}$	$0.0685 \quad 9.70$
droplet (1)	$\begin{pmatrix} 6.88 & -2.62 \\ -2.62 & 25.7 \end{pmatrix}$	$6.52 \quad 26.1$

Fitted second derivatives matrix (dimensionless num. units)

Components diffusion equation

- Use the chain rule and conservation law to obtain the $\partial_t \mu$ eq.

$$\partial_t \left(\frac{\delta \Omega}{\delta \mu^\alpha} \right) = \partial_t \varphi \frac{\partial \left(\delta \Omega / \delta \mu^\alpha \right)}{\partial \varphi} + \sum_{\beta = A,B} \partial_t \mu^\beta \frac{\partial \left(\delta \Omega / \delta \mu^\alpha \right)}{\partial \mu^\beta}$$

$$\partial_t \left(\frac{\delta \Omega}{\delta \mu^\alpha} \right) \propto \partial_t C^\alpha = \nabla \cdot M^{\alpha \beta} \nabla \mu^\beta \qquad \text{for } \alpha = A, B$$

- In the ternary case, becomes linearly coupled w.r.t. ∂_t!

$$\sum_{\beta = A,B} \mathbf{X}^{\alpha \beta} \partial_t \mu^\beta = \nabla \cdot \left(\sum_{\beta = A,B} M^{\alpha \beta} \nabla \mu^\beta \right) - p'(\varphi) \frac{\partial (\omega_0 - \omega_1)}{\partial \mu^\alpha} \partial_t \varphi$$

$$\mathbf{X}^{\alpha \beta} = p(1 - \varphi) \frac{\partial^2 \omega_0}{\partial \mu^\alpha \partial \mu^\beta} + p(\varphi) \frac{\partial^2 \omega_1}{\partial \mu^\alpha \partial \mu^\beta}$$

- **Ternary diffusion couple test-case** — validation of the two-phase three-component sub-model

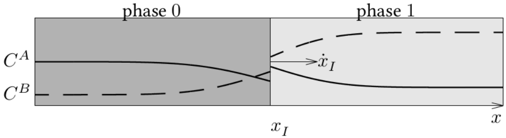

Bulk diffusion, interface conditions

$$\partial_t c^\alpha = \begin{cases} \bar{M}_0^\alpha \nabla^2 \bar{\mu}^\alpha, & -\infty < x < x_I(t), \\ \bar{M}_1^\alpha \nabla^2 \bar{\mu}^\alpha, & x_I(t) < x < +\infty, \end{cases}$$

$$\bar{\mu}^\alpha|_{x_I^-} = \bar{\mu}^\alpha|_{x_I^+} = \bar{\mu}_\pm^\alpha \quad \text{with} \quad \Delta\omega(\mu_\pm^A, \mu_\pm^B) = 0,$$

$$\frac{dx_I}{dt}\left(c^\alpha|_{x_I^-} - c^\alpha|_{x_I^+}\right) = -\left(\bar{M}_0 \partial_x \bar{\mu}^\alpha|_{x_I^-} - \bar{M}_1 \partial_x \bar{\mu}^\alpha|_{x_I^+}\right),$$

$$x_I(t=0) = 0,$$

$$\bar{\mu}^\alpha(t=0,x) = \begin{cases} \bar{\mu}_{-\infty}^\alpha, & -\infty < x < 0, \\ \bar{\mu}_{+\infty}^\alpha, & 0 < x < +\infty, \end{cases}$$

$$\bar{\mu}^\alpha(t, x = \pm\infty) = \bar{\mu}_{\pm\infty}^\alpha.$$

LBM Base algorithm

- Boltzmann-BGK equation in discrete velocity-space $\mathbf{c}_k$

$$f_k(t+\delta t, \mathbf{x}+\mathbf{c}_k\delta t) - f_k(t,\mathbf{x}) = -\frac{\delta t}{\tau}\left[f_k - f_k^{\text{eq}}\right](t,\mathbf{x})$$

- *collision* and *transport* of f_k on the lattice
  - collision: $f_k^* = \left(1-\frac{\delta t}{\tau}\right)f_k + \frac{\delta t}{\tau}f_k^{\text{eq}}$
  - transport: $f_k(t+\delta t, \mathbf{x}+\mathbf{c}_k\delta t) = f_k^*(t,\mathbf{x})$
- $f_k^{\text{eq}} \sim$ expanded Maxwell-Boltzmann distribution

$$f_k^{\text{eq}}(\rho,\mathbf{u}) = w_k\rho\left(1+\frac{\mathbf{c}_k\cdot\mathbf{u}}{c_s^2}+\frac{(\mathbf{c}_k\cdot\mathbf{u})^2}{2c_s^4}-\frac{\mathbf{u}^2}{2c_s^2}\right)$$

Capillary force

Capillary force $\sigma \boldsymbol{\kappa}(\varphi)/W$ normal to the interface with curvature measure

$$\boldsymbol{\kappa}(\varphi) = (3/2)\left(W^2\nabla^2\varphi - f'_{\mathrm{dw}}(\varphi)\right)\nabla\varphi \quad \sim \delta(\mathbf{x}-\mathbf{x}_I)\,\kappa\,\mathbf{n}$$